


RESEARCH ARTICLE

Lost in space(s): Multimodal neuroimaging of disorientation along the Alzheimer's disease continuum

Gregory Peters-Founshtein^{1,2}  | Lidor Gazit^{1,3} | Tahel Naveh^{1,3} |
Liran Domachevsky^{2,4} | Amos D. Korczyn⁵ | Hanna Bernstine^{4,6,7} |
Limor Shaharabani-Gargir⁴ | David Groshar^{4,6} | Gad A. Marshall⁸ | Shahar Arzy^{1,3}

¹The Computational Neuropsychiatry Lab, Department of Medical Neurobiology, Faculty of Medicine, Hebrew University of Jerusalem, Jerusalem, Israel

²Department of Nuclear Medicine, Sheba Medical Center, Ramat-Gan, Israel

³Department of Neurology, Hadassah Hebrew University Medical School, Jerusalem, Israel

⁴Department of Nuclear Medicine, Assuta Medical Center, Tel-Aviv, Israel

⁵Department of Neurology, Tel-Aviv University, Tel-Aviv, Israel

⁶Department of Imaging, Tel-Aviv University, Tel-Aviv, Israel

⁷Department of Nuclear Medicine, Rabin Medical Center, Petah Tikva, Israel

⁸Department of Neurology, Center for Alzheimer Research and Treatment, Harvard Medical School, Brigham and Women's Hospital, Massachusetts General Hospital, Boston, Massachusetts, USA

Correspondence

Gregory Peters-Founshtein, Department of Nuclear Medicine, Sheba Medical Center, Ramat-Gan, Israel.

Email: gregory.founshtein@mail.huji.ac.il

Funding information

National Institutes of Health, Grant/Award Number: R21 AG070877; Israeli Science Foundation, Grant/Award Number: 3213/19

Abstract

Orientation is a fundamental cognitive faculty and the bedrock of the neurologic examination. Orientation is defined as the alignment between an individual's internal representation and the external world in the spatial, temporal, and social domains. While spatial disorientation is a recognized hallmark of Alzheimer's disease (AD), little is known about disorientation beyond space in AD. This study aimed to explore disorientation in spatial, temporal, and social domains along the AD continuum. Fifty-one participants along the AD continuum performed an ecological orientation task in the spatial, temporal, and social domains while undergoing functional MRI. Disorientation in AD followed a three-way association between orientation domain, brain region, and disease stage. Specifically, patients with early amnesic mild cognitive impairment exhibited spatio-temporal disorientation and reduced brain activity in temporoparietal regions, while patients with AD dementia showed additional social disorientation and reduced brain activity in frontoparietal regions. Furthermore, patterns of hypoactivation overlapped different subnetworks of the default mode network, patterns of fluorodeoxyglucose hypometabolism, and cortical atrophy characteristic of AD. Our results suggest that AD may encompass a disorder of orientation, characterized by a biphasic process manifesting as early spatio-temporal and late social disorientation. As such, disorientation may offer a unique window into the clinicopathological progression of AD.

This is an open access article under the terms of the [Creative Commons Attribution-NonCommercial-NoDerivs](https://creativecommons.org/licenses/by-nc-nd/4.0/) License, which permits use and distribution in any medium, provided the original work is properly cited, the use is non-commercial and no modifications or adaptations are made.

© 2024 The Authors. *Human Brain Mapping* published by Wiley Periodicals LLC.

Significance statement

Despite extensive research into Alzheimer's disease (AD), its core cognitive deficit remains a matter of debate. In this study, we investigated whether orientation, defined as the ability to align internal representations with the external world in spatial, temporal, and social domains, constitutes a core cognitive deficit in AD. To do so, we used PET-fMRI imaging to collect behavioral, functional, and metabolic data from 51 participants along the AD continuum. Our findings suggest that AD may constitute a disorder of orientation, characterized by an early spatio-temporal disorientation and followed by late social disorientation, manifesting in task-evoked and neurodegenerative changes. We propose that a profile of disorientation across multiple domains offers a unique window into the progression of AD and as such could greatly benefit disease diagnosis, monitoring, and evaluation of treatment response.

KEYWORDS

Alzheimer's disease, functional magnetic resonance imaging, mild cognitive impairment, orientation, social, space, time

1 | INTRODUCTION

Orientation is a fundamental cognitive faculty, allowing the behaving self to link his/her current state to their internal representations of the external world (Berrios, 1982; Peer et al., 2015). Commonly, orientation is evaluated in the spatial, temporal, and social domains, and as such, it is recognized as the bedrock of the cognitive clinical evaluation (Mahendran et al., 2015; Rapoport & Rapoport, 2015). Nonetheless, standard evaluations of orientation are limited to testing only the patient's knowledge about the present time, current location, and personal identity, resulting in low sensitivity to early cognitive decline (Peters-Founshtein et al., 2018).

In recent years, several lines of research (Coughlan et al., 2018; Delpolyi et al., 2007; Kunz et al., 2015; Peters-Founshtein et al., 2018) have demonstrated that spatial orientation is potentially affected early on by AD pathology. One such study (Coughlan et al., 2019) used the Sea Hero Quest (SHQ) spatial navigation paradigm to compare young, cognitively intact, heterozygote carriers of apolipoprotein E (apo)- $\epsilon 4$ alleles ($\epsilon 3/\epsilon 4$), a known risk multiplier of AD to demographically matched healthy homozygote, $\epsilon 3/\epsilon 3$, participants. Comparing the two groups as they perform several goal-oriented wayfinding tasks revealed significant disruptions in navigation performance in people at risk for AD showing no clinically detectable cognitive deficits. However, orientation is not restricted to the spatial domain. It involves other domains such as the temporal and social ones (Du et al., 2021; Peer et al., 2015) that have been shown to be progressively impaired along the AD continuum (Dafni-Merom et al., 2019; Peters-Founshtein et al., 2018). Moreover, tests of orientation have been found to better discriminate between cognitively normal (CN) and amnesic mild cognitive impairment (amCI) participants (95% accuracy) when compared to standard neuropsychological evaluations (Addenbrooke's Cognitive Examination (ACE)—71%; Mini-Mental State Examination (MMSE)—70%) (Peters-Founshtein

et al., 2018). This superiority may stem from a considerable overlap between the patterns of orientation-evoked brain activity and patterns of AD neurodegeneration (Peters-Founshtein et al., 2018).

Independently, the pattern of orientation-evoked brain activity was found to markedly overlap with the default mode network (DMN) (Hayman & Arzy, 2021; Peer et al., 2015; Peters-Founshtein et al., 2018). The DMN is a network of interconnected brain regions, active when individuals engage in self-referential tasks such as autobiographical memory retrieval and personal future planning (Andrews-Hanna et al., 2010). Furthermore, AD neuropathology (amyloid- β [$A\beta$] and tau) has been shown to carry increased probability of spreading within rather than outside of the DMN (Buckner et al., 2005; Franzmeier et al., 2020). Subsequent studies, re-evaluating DMN homogeneity, have suggested the DMN to be comprised of partially dissociated components, each underlying different cognitive functions (Andrews-Hanna et al., 2010; Barnett et al., 2014, 2021; Buckner & DiNicola, 2019). These components have been denoted as DMN A, including the ventromedial prefrontal cortex, the posterior cingulate cortex, and parts of the temporoparietal junction; DMN B, including the dorsomedial prefrontal cortex, the lateral temporal cortex, parts of the temporoparietal junction, and the temporal pole; and DMN C, including the hippocampus, the parahippocampal cortex, the retrosplenial cortex, and parts of the temporoparietal junction. While the functional differentiation between components is still being investigated, one meta-analysis has associated each subnetwork with distinctive cognitive processes (Andrews-Hanna et al., 2014). In this view, DMN A facilitates self-related, emotional, and social processes, enabling the extraction of personal meaning from salient information; DMN B supports the retrieval of semantic and conceptual knowledge; and DMN C supports mnemonic and spatio-temporal processes and is thought to provide episodic context and aid in constructing mental simulations. Taken together, the overlapping patterns of DMN connectivity and orientation in space, time, and person imply a latent

model of inter-related neuropathological and cognitive changes in AD (Buckner et al., 2005).

In the current comprehensive study, we aimed to evaluate the relations between (1) spatio-temporal and social disorientation, (2) DMN subnetworks, and (3) neurodegeneration, in individuals along the AD continuum, using positron emission tomography (PET)-functional magnetic resonance imaging (fMRI). Considering the neuropsychological profile of AD-related cognitive decline (early spatio-temporal and later social decline), jointly with multiple studies suggesting a segregation between spatio-temporal and social processing in the brain, we hypothesized that spatio-temporal and social orientation would be differently affected along the AD continuum. Hence, we set to test and characterize these differences in behavioral performance and brain activity in the context of DMN topology and patterns of AD-related neurodegeneration.

2 | METHODS

2.1 | Participants

Fifty-one individuals (27 females, mean age 71.43 ± 0.82 ; for detailed demographics, see Table 1) participated in the study. Twenty-three patients with amnesic MCI were the main focus of the study (Cohen's $d > 0.8$) and compared to 12 patients with AD dementia and 16 age-matched CN older adults. Participants underwent a complete neurologic examination, cerebrovascular risk factor assessment using the Hachinski Ischemic Scale (Hachinski et al., 1975), and a comprehensive neuropsychological evaluation that included the Clinical Dementia Rating (Morris, 1993), Montreal Cognitive Assessment (Nasreddine et al., 2005), ACE (Mathuranath et al., 2000), and Frontal Assessment Battery (Dubois et al., 2000). All participants underwent structural T1- and T2-weighted MRI and fluorodeoxyglucose (FDG)-PET, which were reviewed by neuroradiology and nuclear medicine specialists to exclude non-AD etiologies.

Criteria for inclusion of CN participants were as follows: (1) no active neurologic or psychiatric disorders, (2) if medical problems were present, the illnesses or their treatments did not interfere with cognitive function, (3) a normal neurologic examination, and (4) independently functioning community dwellers.

Cognitively impaired participants met the National Institute on Aging and the Alzheimer's Association clinical criteria for AD dementia or aMCI (Albert et al., 2011; McKhann et al., 2011). Criteria for inclusion of aMCI participants were as follows: (1) memory complaint, corroborated by an informant, (2) objective memory impairment for age and education, (3) largely normal general cognitive function, (4) essentially intact activities of daily living, and (5) not demented.

All AD patients recruited for this study had a Clinical Dementia Rating (CDR) score of ≥ 1.0 and MMSE score of ≥ 20 .

Exclusionary criteria included a history of major traumatic brain injury, other known neurologic disease or insult, neurologic focal signs, evidence for ischemic or other neurologically significant lesions (as assessed by MRI), use of antipsychotic medications or barbiturates, previous diagnosis of bipolar disorder or schizophrenia, use of anti-Parkinsonian, anticonvulsant, or medications with anticholinergic side effects, history of drug or alcohol abuse, severe trauma preventing normal use of hands (needed to press buttons), clinical depression or anxiety (unless medically controlled for >2 years), lack of capacity to give informed consent, and unwillingness or inability to participate in the study.

All participants had adequate visual and auditory acuity and a Hachinski Ischemic Score of ≤ 4 . All participants provided written informed consent prior to undergoing study procedures, and the study was approved by the ethics committee of the Assuta Medical Center.

2.2 | Experimental stimuli

Stimuli used in the task consisted of personally familiar names of places, events, and people. To minimize the effects of memory

TABLE 1 Demographics and neuropsychological assessment scores.

	CN	aMCI	AD dementia
Gender (F M)	9 7	14 9	4 8
Age (years)	69.5 ± 1.2 (57–80)	73.13 ± 1.38 (61–87)	70.75 ± 1.91 (63–79)
Education (years)	17.31 ± 0.8	16.45 ± 1	14.5 ± 1.31
MMSE ^{a,b,c}	29 ± 0.24	26.72 ± 0.46	21.86 ± 1.1
ACE ^{a,b,c}	94.78 ± 1	85.71 ± 1.61	66.46 ± 3.9
MoCA ^{a,b,c}	28.63 ± 0.38	24.72 ± 0.52	18.5 ± 1.33
CDR global ^{a,b,c}	0.21 ± 0.06	0.57 ± 0.05	1.17 ± 0.19
Katz index	6 ± 0	5.86 ± 0.34	5.17 ± 1.27

Note: All values represent the mean \pm standard error of the mean (SEM).

Abbreviations: ACE, Addenbrooke's Cognitive Examination; CDR, Clinical Dementia Rating; Katz index of independence in activities of daily living (ADL); MMSE, Mini-Mental State Examination; MoCA, Montreal Cognitive Assessment.

^aStatistical significance ($p < .05$) between CN and AD dementia.

^bStatistical significance ($p < .05$) between CN and MCI.

^cStatistical significance ($p < .05$) between CN and MCI.

disruptions on orientation testing, a set of personally familiar stimuli was obtained from each participant prior to testing. Participants were presented with a list of potential stimuli and for each were asked to approximate its location (for space stimuli) or year (for time stimuli). Failing to reference both the relevant region of the country and at least one nearby landmark (space) or miscalculating the correct year (time) resulted in the removal of the specific stimulus from further testing. In addition, participants were asked to generate a list of 8 close family members, 8 friends, and 8 acquaintances, which was corroborated with either a child or spouse (for additional details, see Appendix S1).

2.3 | Experimental procedure—fMRI task

In the orientation task, participants were presented with pairs of familiar stimuli consisting of names of either two cities in Israel, two events, or two people and were asked to determine which of the two is closer to them: geographically closer to their current location for cities, chronologically closer to the present time for events, or personally closer to them for people. To standardize experimental sessions based on personalized sets of stimuli, stimuli were split into three distance categories. Trials were generated by pairing stimuli from adjacent distance categories only. Stimuli were presented using the Presentation software (version 18.0, Neurobehavioral Systems, Inc., Berkeley, CA; for additional details, see Appendix S1).

Trials were presented in a randomized block design, with each block containing three consecutive trials belonging to a specific domain and distance category. Each trial was presented for a maximum of 10 s. Experiments consisted of four experimental runs, each containing 12 three-trial blocks in randomized order, balanced for both domain and distance categories. Additionally, participants performed a lexical control task in two additional separate runs. In the lexical control task, participants were presented with stimuli pairs from the same sets but were instructed to indicate which of the words contains the letter “A.” Stimuli were presented using the Presentation software (version 18.0; Neurobehavioral Systems, Inc., Berkeley, CA). Prior to the experiment, a 5-min training task containing different stimuli was administered. See Appendix S1 for more details. The task was modeled on our previous studies of orientation (Dafni-Merom et al., 2019; Hayman & Arzy, 2021; Peer et al., 2015; Peters-Founshstein et al., 2018).

2.4 | Statistical analyses

Efficacy scores (ESs) (Townsend & Ashby, 1983) were computed for each participant and domain separately by calculating the ratio between the success rate (SR) and mean response time (RT). A global ES was calculated for each participant by averaging the ESs across the three domains. Subsequently, mean ESs were compared across the three groups (AD dementia, aMCI, and CN) using analysis of variance (ANOVA) and Tukey–Kramer post hoc tests. For the neuropsychological tests, scores were recorded according to the relevant testing guidelines.

2.5 | MRI and PET data acquisition and preprocessing

For details regarding MRI and FDG-PET data acquisition and preprocessing, refer to Appendix S1.

2.6 | PET analysis

To correct for AD-unrelated variance, FDG standardized uptake values (SUVs) were first normalized by mean cerebellar GM SUV, to produce SUV ratio (SUVr) maps (Marcus, Mena, & Subramaniam, 2014). We then constructed a GLM to compare glucose uptake between the CN, aMCI, and AD dementia groups. Specifically, we performed voxel-wise two-sample *t*-tests comparing SUVr values between the three clinical contrasts (CN–aMCI, aMCI–AD dementia, and CN–AD dementia), with age, years of education, and gender included as nuisance variables (Figure S1A) (Kanda et al., 2008).

2.7 | Voxel-based morphometry

We applied voxel-based morphometry (VBM) analysis to compare gray matter (GM) density between CN, aMCI, and AD dementia groups (Ashburner & Friston, 2000). Specifically, we used a general linear model (GLM) (Worsley & Friston, 1995) to perform voxel-wise two-sample *t*-test for each of the clinical contrasts (CN–aMCI, aMCI–AD dementia, and CN–AD dementia), with age, years of education, gender, and total intracranial volume included as nuisance variables (see Figure S1B). Here, and in all further analyses, we applied a false discovery rate (FDR) correction for multiple comparisons ($p < .05$) and cluster size thresholding of 20 voxels. All analyses were performed using the statistical parametric mapping (SPM) 12 software package (version 7219) and in-house MATLAB scripts (version 2019b; MathWorks, Natick, MA, USA). In-house scripts are publicly available (<https://www.neuropsychiatrylab.com/codes>).

2.8 | Identification of orientation-evoked activity

To assess the selective activations elicited by different experimental conditions, we applied a group-level random-effects GLM analysis using data from all participants. To isolate orientation-specific activity, we contrasted the (1) spatial and temporal conditions (spatio-temporal) and, separately, the (2) social condition with the lexical control task (Peer et al., 2015).

2.9 | Orientation task analysis

We used a group-level random-effects GLM to compare spatio-temporal and social evoked activations between the CN, aMCI, and AD dementia groups. Specifically, we performed voxel-wise two-sample *t*-tests comparing task parameter estimates of each domain in

the three clinical contrasts with age, years of education, and gender included as nuisance variables. To exclude non-specific activations, maps of task over lexical control in all participants served as inclusive masks.

2.10 | Region-of-interest (ROI) analysis

To associate task-evoked patterns of brain activity and glucose metabolism in the brain with DMN topology, ROIs for DMN subnetworks A, B, and C were extracted from the Schaefer 200 atlas (Schaefer et al., 2018). DMN ROIs were used to compare GM density, glucose uptake (Figure S2), and task-evoked activity (parameter estimates of space-time and person over rest) between CN, aMCI, and AD dementia groups. ANOVA and the Tukey-Kramer post hoc test were used in all the comparisons.

2.11 | Mediation analysis

We set to test the hypothesis that neurodegeneration, expressed as changes in glucose metabolism, accounts for some of the shared variance between orientation-evoked activity and orientation performance along the AD continuum. For this purpose, we conducted a whole-brain voxel-wise mediation analysis using the Bootstrap Regression Analysis of Voxelwise Observations (BRAVO) toolbox (<https://sites.google.com/site/bravotoolbox>). Two three-path models were constructed, separately for spatio-temporal and social tasks (see Figure 4a), with parameter estimates for task over rest as the predictor variable (“X” in Figure 4a), task ES as an outcome variable (“Y” in Figure 4a), and FDG-SUVr as the mediator variable (“M” in Figure 4a). The mediation analysis tested whether the relation (path c) between the predictor variable (“X,” space-time/person beta) and an outcome variable (“Y,” space-time/person ES) is significantly attenuated when the relation between X and a mediator variable (“M,” FDG-SUVr) (path a) and the relation between M and Y (path b) are added to the model (Figure 4a). Mediation effect sizes were computed for every voxel. Significance was assessed through a permutation procedure with 10,000 iterations and corrected through FDR for voxel-wise multiple comparisons. Importantly, models were applied to all participants and were agnostic to the clinical labels. To test the specificity of the mediation-related effects for the orientation tasks, we repeated the above analysis for the space-time and person domains of the lexical control task (Figure S3).

2.12 | Permutation analysis for overlap significance

We performed overlap analysis to assess the correspondences between DMN A, DMN B, and DMN C ROIs; spatio-temporal and social orientation-evoked maps of activity (Figure 3); spatio-temporal and social maps of mediation (Figure 4); and clinical

contrasts for VBM (Figure S1) and FDG-SUVr (Figure S1). To assess overlap, we quantified the shared number of suprathreshold (orientation, mediation, VBM, and FDG) and DMN ROI voxels and divided by the total number of DMN ROI voxels. To determine significance of overlap, we used a permutation analysis. We generated 10,000 permutation maps in which the same number of suprathreshold voxels was randomly shuffled and then calculated the proportion of permutation maps in which the shared number of voxels was equal to or greater than the overlap between the original masks. This effectively determined the probability of observing the level of overlap we found with a random pattern of suprathreshold parameter.

3 | RESULTS

3.1 | Spatio-temporal and social orientation performance is differently affected along the AD continuum

Behavioral results for the orientation task across all domains showed significant differences between the three clinical groups ($p < .05$, ANOVA and Tukey-Kramer post hoc test). Participants with AD dementia scored significantly lower than participants with aMCI, and the latter scored lower than CN participants (mean \pm standard error of the mean (SEM): 0.17 ± 0.02 [s^{-1}], 0.32 ± 0.021 [s^{-1}], 0.41 ± 0.02 [s^{-1}]; Figure 1a) unlike the lexical control task (mean \pm SEM: 0.4 ± 0.07 [s^{-1}], 0.68 ± 0.04 [s^{-1}], 0.82 ± 0.06 [s^{-1}]; Figure 1b). Efficacy scores (ESs) in the spatio-temporal domains (mean \pm SEM: 0.15 ± 0.02 [s^{-1}], 0.29 ± 0.02 [s^{-1}], 0.38 ± 0.02 [s^{-1}]; Figure 1c) showed significant differences between all 3 clinical groups (AD dementia, aMCI, and CN, respectively; $p < .05$). ES in the social domain (mean \pm SEM: 0.21 ± 0.03 [s^{-1}], 0.42 ± 0.02 [s^{-1}], 0.48 ± 0.02 [s^{-1}]; Figure 1d) showed significant differences only between AD dementia and non-AD participants (CN and aMCI), comparable with the lexical task.

3.2 | Divergent changes in spatio-temporal and social activity along the AD continuum

Spatio-temporal orientation was shown to activate the precuneus, parieto-occipital sulcus, anterior and posterior cingulate cortices, parahippocampal and supramarginal gyri bilaterally, and the left superior frontal gyrus (Figure 2a). Social orientation activated the anterior and posterior cingulate cortices, the angular and superior medial gyri, and the putamen bilaterally (Figure 2a). Subsequent second-level GLM analysis revealed significant differences in spatio-temporal orientation between CN and aMCI participants and CN and AD dementia participants in the precuneus, posterior cingulate cortex, parahippocampal gyri, and hippocampus bilaterally (Figure 2b). Second-level GLM analysis of social orientation showed significant differences between aMCI and AD dementia participants and between CN and AD dementia

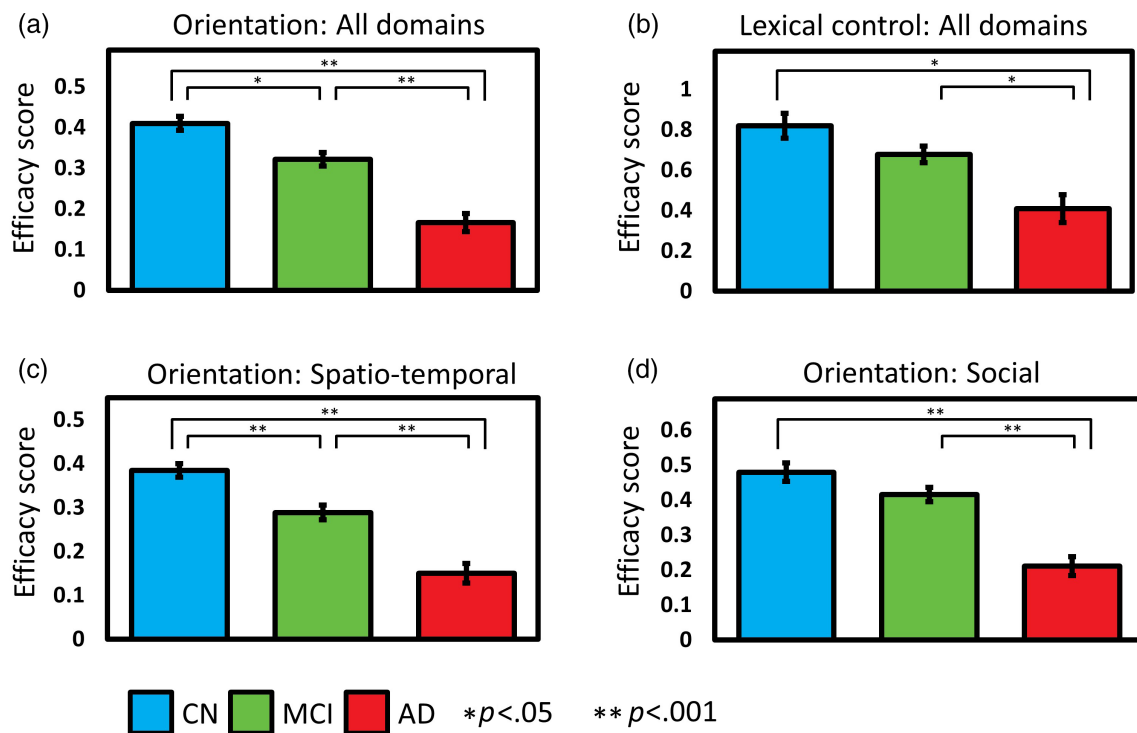


FIGURE 1 Spatio-temporal and social orientation changes along the AD continuum. Mean efficiency scores (ESs) and standard error of the mean (SEM) of CN ($N = 16$, blue), MCI ($N = 23$, green), and AD dementia ($N = 12$, red) participants for the orientation task in all domains (a), the lexical control task in all domains (b), and the orientation task in spatio-temporal (c) and social (d) domains. Significant CN–MCI differences were found in all domain orientation (a; $p < .05$) and space and time orientation (c; $p < .001$). Significant MCI–AD dementia and CN–AD dementia differences were found in all domains, spatio-temporal and social orientation task ES (a, c, d; $p < .001$), as well as in the lexical task (b; $p < .05$). Statistical significance was estimated using ANOVA and Tukey–Kramer post hoc test.

participants in the precuneus, superior medial, and angular gyri bilaterally (Figure 2c).

3.3 | Spatio-temporal and social orientation-evoked activity overlaps differently with default mode subnetworks

To examine whether discrete brain networks underlie spatio-temporal and social orientation, we overlapped suprathreshold task-evoked activation maps with DMN A, DMN B, and DMN C ROIs. Spatio-temporal orientation activity was found to significantly overlap the DMN C (27%, $p < .001$, Figure 3a,b). Social orientation activations were found to significantly overlap the DMN A (28%, $p < .001$) and DMN B (11%, $p < .001$, Figure 3a,b). We then compared mean task-evoked coefficient estimated for spatio-temporal and social orientation among the CN, aMCI, and AD dementia groups, in each of the DMN ROIs. DMN ROI analysis for the spatio-temporal orientation showed differences between CN and aMCI and AD dementia participants in DMN C only ($p < .05$, Figure 3c and Figure S2A). For social orientation, DMN ROI analysis showed differences between AD dementia participants and aMCI and CN participants in DMN A and DMN B only ($p < .05$, Figure 3c and Figure S2B).

3.4 | AD-related hypometabolism mediates the relations between orientation performance and orientation-evoked activity

Spatio-temporal mediation effects were found to be significant ($p < .05$, FDR corrected) in the parahippocampal gyrus, posterior cingulate cortex, and precuneus, significantly overlapping DMN A (7%, $p < .001$, Figure 4c) and DMN C (17%, $p < .001$, Figure 4c). Social mediation effects were found to be significant in the precuneus ($p < .05$, FDR corrected), significantly overlapping with DMN A (7%, $p < .001$, Figure 4c) and DMN C (8%, $p < .001$, Figure 4c). Mediation analysis for the lexical control task in space–time revealed small overlap with DMN C (1%, $p < .001$, Figure S3B,C). Social lexical mediation analysis revealed small overlap with DMN A (3%, $p < .001$, Figure S3B2,C2).

4 | DISCUSSION

Our study revealed that an early stage of AD-related decline, aMCI, manifests in spatio-temporal disorientation and task-evoked hypoactivation in temporoparietal regions, significantly overlapping the DMN C subnetwork. Participants at the later stage of AD dementia

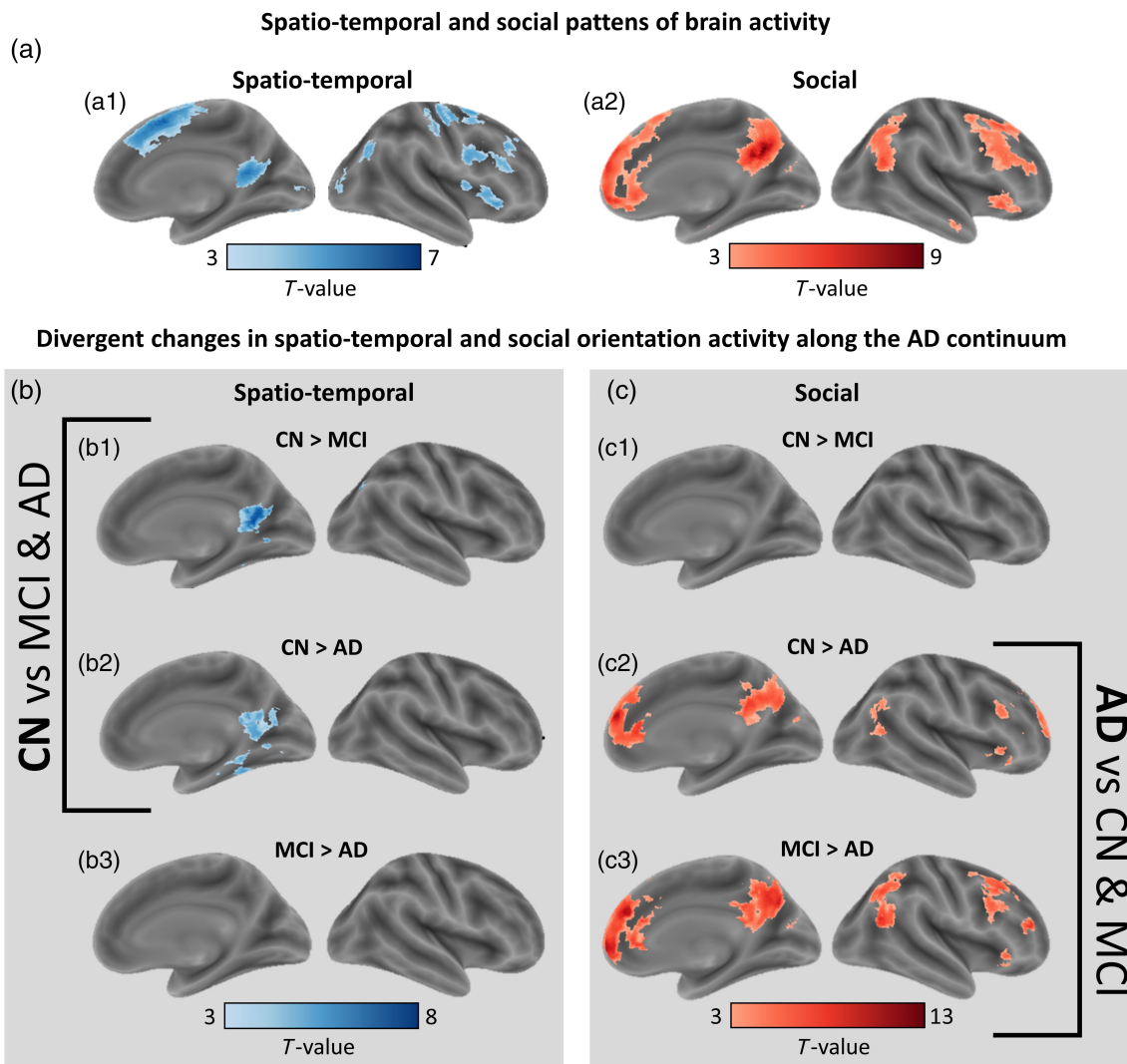


FIGURE 2 Changes in spatio-temporal and social orientation activity in AD. (a) Spatio-temporal and social patterns of brain activity. Results of GLM analysis exhibiting contrast maps of spatio-temporal (a1) and social (a2) orientation tasks over the lexical control task (all participants, degrees of freedom [df] = 50, $p < .05$ FDR corrected, cluster size >20 voxels). (b, c) Divergent changes in spatio-temporal and social orientation activity. Spatio-temporal (b) and social (c) disorientation contrasted task-evoked activity maps across the three clinical groups: CN greater than MCI participants in spatio-temporal (b1) and social (c1) orientation (df = 38, $p < .05$ FDR corrected, cluster size thresholding of 20 voxels); CN greater than AD dementia participants in spatio-temporal (b2) and social (c2) orientation (df = 34, $p < .05$ FDR corrected, cluster size thresholding of 20 voxels); and MCI greater than AD dementia participants in spatio-temporal (b3) and social (c3) orientation (df = 27, $p < .05$ FDR corrected, cluster size thresholding of 20 voxels).

exhibited social disorientation and task-evoked hypoactivation in frontoparietal regions, significantly overlapping the DMN A subnetwork. Moreover, the changes in task-evoked brain activity followed the pattern of glucose hypometabolism. Mediation analysis showed hypometabolism to mediate the relations between orientation-evoked activity and task performance along the AD continuum.

The DMN is a network of interconnected brain regions, which includes medial prefrontal, posterior cingulate, and hippocampal brain structures. The DMN is known to activate when individuals engage in self-referential tasks, such as autobiographical memory retrieval and future planning (Buckner & DiNicola, 2019). In AD, early works have demonstrated a high degree of overlap between maps of DMN connectivity and patterns of structural and

metabolic disruptions, as well as A β and tau deposition (Buckner et al., 2005; Palmqvist et al., 2017). More specifically, in AD patients, functionally connected regions were found to correlate with tau accumulation rates (Franzmeier et al., 2020), corroborating the hypothesis that DMN connectivity facilitates trans-synaptic dispersion of tau across the brain (Buckner et al., 2005; Franzmeier et al., 2020). Independently, several works have shown the DMN to comprise several distinct subnetworks (Andrews-Hanna et al., 2010; Buckner & DiNicola, 2019). The detailed organization of these networks is revealed both in group-level and single-subject-level analyses. Evidence emerging from such studies suggests that the DMN comprises two or three separate networks with clear spatial distinctions.

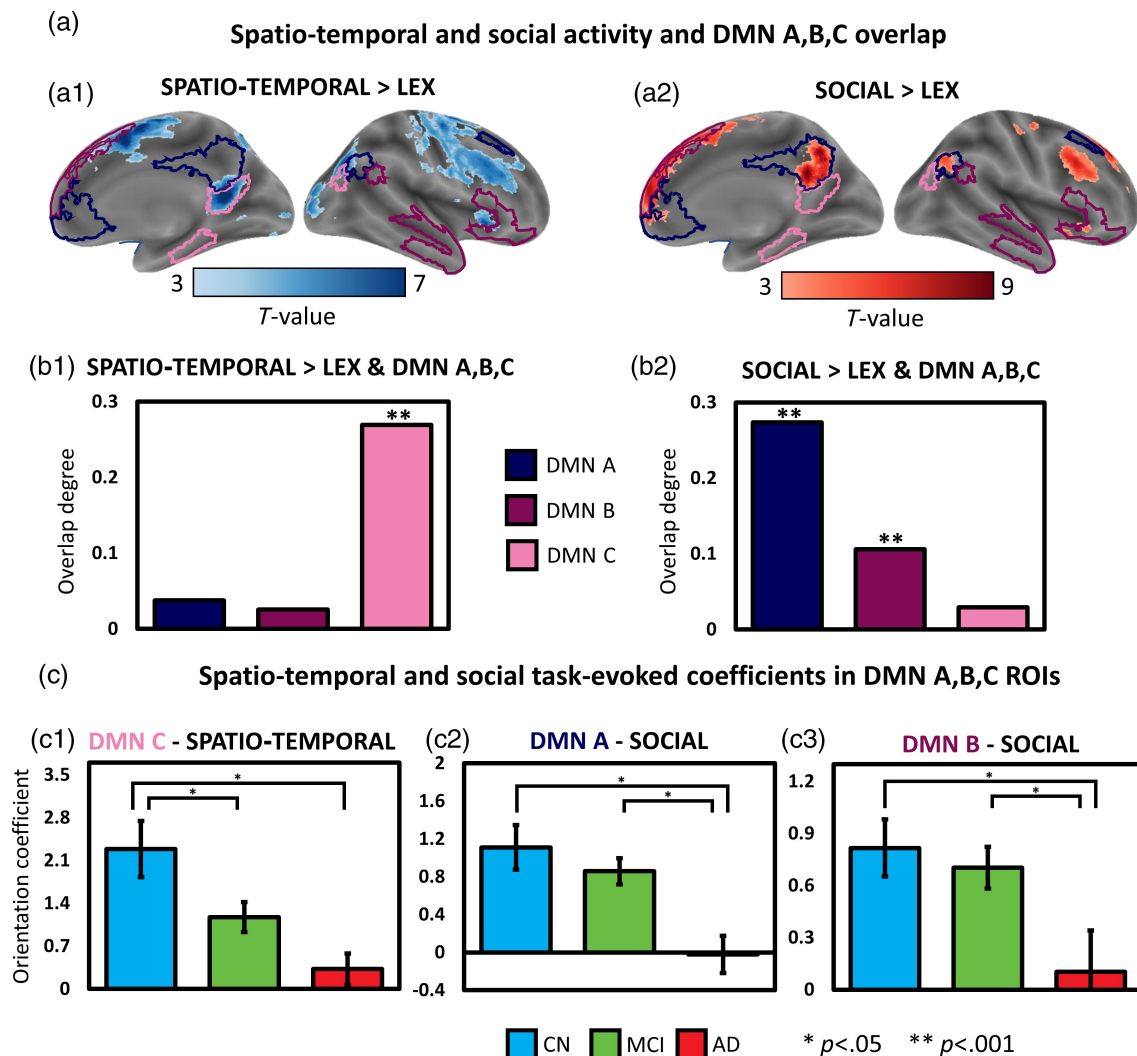


FIGURE 3 Orientation-evoked activity overlaps default mode subnetworks differently. (a) Spatio-temporal and social activity and DMN A, DMN B, and DMN C overlap. Delineations of DMN subnetworks (Schaefer et al., 2018) DMN A (dark), DMN B (medium), and DMN C (light) superimposed on maps of spatio-temporal (a1) and social (a2) orientation tasks (orientation > lexical control; all participants, $df = 50$, $p < .05$ FDR corrected, cluster size >20 voxels). (b) The percent of overlap between suprathreshold task-evoked spatio-temporal (b1) and social (b2) maps and DMN subnetworks A, B, and C. Asterisks indicate significant overlap (permutation test, 10,000 iterations). (c) Spatio-temporal and social task-evoked coefficients in DMN A, DMN B, and DMN C ROIs. Mean GLM-derived parameter estimates for spatio-temporal (c1) and social (c2 and c3) orientation (>rest) in significantly overlapping (b) DMN subnetworks (c1—DMN C—spatio-temporal; c2—DMN A—social; c3—DMN B—social) for CN ($N = 16$, blue), MCI ($N = 23$, green), and AD dementia ($N = 12$, red). Significant differences were found between CN and AD dementia participants in DMN A, DMN B, and DMN C, between MCI and AD dementia participants in DMN A and DMN B, and between CN and MCI participants in DMN C (ANOVA and Tukey–Kramer post hoc test, $p < .05$).

Here, we demonstrated the association between DMN subnetworks and spatio-temporal and social orientation in AD. Specifically, our findings suggest that disorientation, manifesting as progressive disruptions in behavioral performance and task-evoked brain activity, is linked to sequential disruption in DMN C (early) and DMN A (late) regions along the AD continuum. Jointly, these results raise the possibility that DMN subnetworks are associated with distinct phases in AD progression.

Additional sources of evidence offer complementary accounts of the roles DMN subnetworks potentially play in AD pathology. PET neuroimaging of the two molecular AD hallmarks, A β and tau, has

revealed distinct patterns of deposition across the brain. A β initially accumulates in medial parietal regions and spreads from neocortex to allocortex to brainstem. Tau, by contrast, first becomes evident in the entorhinal cortex, from which it spreads to limbic areas and from there to the neocortex. In early stages of the disease, the pattern of A β deposition markedly overlaps with DMN A, while tau deposition markedly overlaps with DMN C (van der Kant et al., 2020). Jointly, the associations between A β , tau, and DMN subnetworks and our findings, showing early DMN C and late DMN-A hypometabolism, may suggest that at later stages of the disease, A β accumulation in DMN A facilitates the spread of tau beyond DMN C brain regions (Busche &

(a) Schematic of mediation model of brain activity, glucose metabolism, and orientation performance

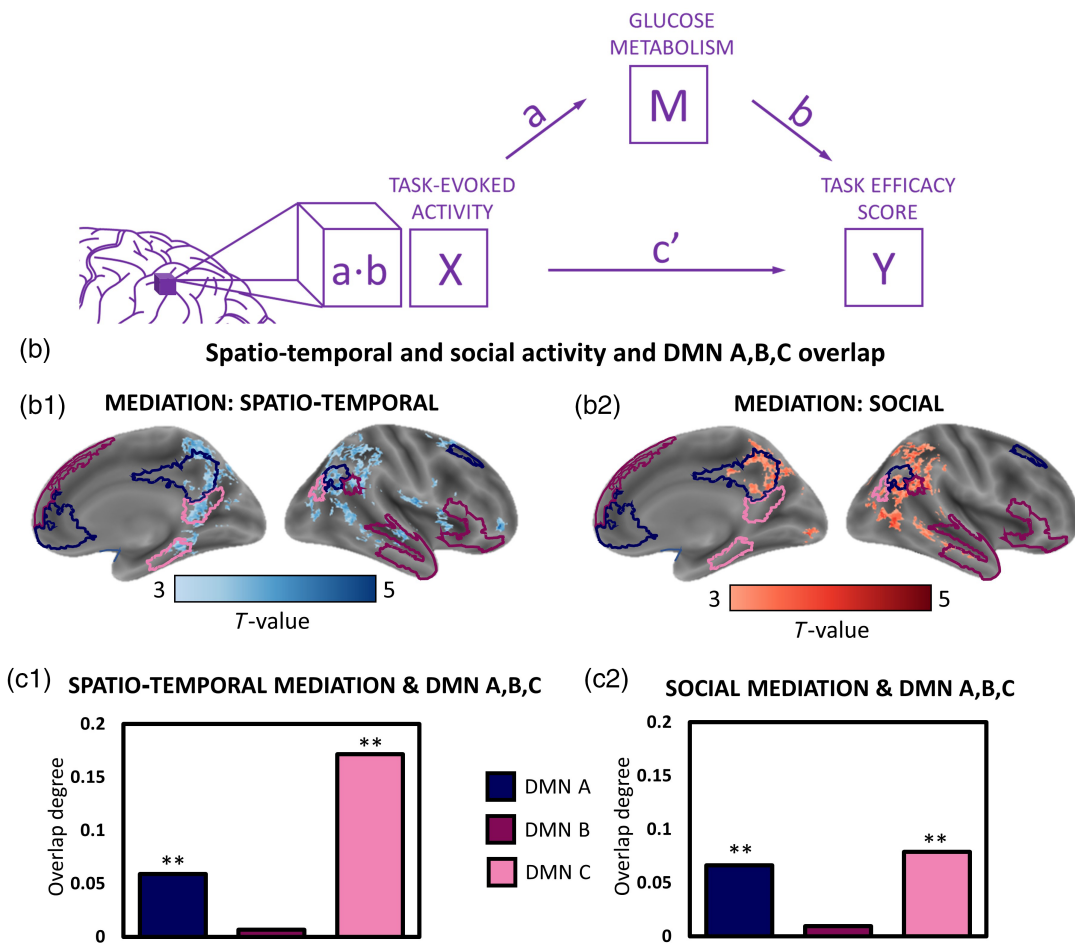


FIGURE 4 Mediation models of brain activity, glucose metabolism, and orientation performance. (a) Mediation analysis was used to test the hypothesis that changes in FDG-PET uptake (M) across the AD continuum alter the relations between spatio-temporal (b1) and social (b2) orientation-evoked brain activity (X) and orientation task performance (y). (b) Spatio-temporal and social mediation and DMN A, DMN B, and DMN C overlap. Delineations of DMN subnetworks (Schaefer et al., 2018) DMN A (dark), DMN B (medium), and DMN C (light) superimposed on maps of spatio-temporal (b1) and social (b2) mediation ($p < .05$, FDR corrected). (c) The percent of overlap between suprathreshold task-evoked spatio-temporal (c1) and social (c2) suprathreshold mediation maps and DMN subnetworks A, B, and C. Asterisks indicate significant overlap (permutation test, 10,000 iterations).

Hyman, 2020). As $A\beta$ was independently shown to affect functional connectivity (Lin et al., 2020), it is possible that $A\beta$ facilitates tau spread beyond DMN C regions by altering DMN A/C connectivity. This hypothesis is supported by the discovery of primary age-related tauopathy (PART), a neuropathological entity defined by the presence of tau in the absence of $A\beta$, which has been characterized by (1) tau remaining confined to the MTL regions and (2) appearing in cognitively intact older adults (Crary et al., 2014). As the nature of the relationship between $A\beta$ and tau eludes consensus, the prospect of functional connectivity, specifically between subnetworks of the DMN, could potentially inform the mechanisms of propagation of AD neuropathology across the brain.

Our findings not only mark the significance of orientation testing in AD but also may suggest a role for AD as a potential neurodegenerative disease model of disorientation. From this perspective, our results may contribute to the enduring question of domain-specific

(Silson et al., 2019) versus domain-general (Park et al., 2021) systems of orientation. Coinciding with previously published findings (Silson et al., 2019), here we linked spatio-temporal and social processing with temporoparietal and frontoparietal regions, respectively. The diverging patterns of activity and vulnerability along the AD continuum for spatio-temporal and social orientation suggest a domain-dedicated framework, with its various components sequentially affected along the AD continuum.

However, several studies have challenged this paradigm of spatio-temporal and social dedicated brain regions, showing that, under some conditions, temporoparietal regions are involved in social domain tasks and frontoparietal regions are involved in spatial tasks. As a possible way of reconciling these seemingly contradictory findings, we propose that spatio-temporal and social activations represent special cases of archetypical modes of information processing (Kaplan & Friston, 2019; Whittington et al., 2022), underlying

temporoparietal (DMN C) and frontoparietal (DMN A) regions, respectively (Byrne et al., 2007; Whittington et al., 2022). Specifically, DMN C regions were proposed to prioritize relational information, while DMN A regions were found to accentuate self-referential aspects of the experience. In our task, relational and self-referential processes are associated with spatio-temporal and social orientation, respectively; however, under different task conditions, these associations could potentially shift. In future studies, we intend to generalize beyond specific tasks and define the underlying cognitive roles of the DMN subnetworks.

Social engagement in AD has been explored from several perspectives (Bennett et al., 2006; Fredericks et al., 2018; Sabat & Lee, 2012; Sturm et al., 2013). One approach focuses on disruptions in social mapping and orientation, that is, the ability to mentalize relational representation of other people within a multi-dimensional (social) space (Schafer & Schiller, 2018). Here, we demonstrate the relative resilience of social orientation, which finally breaks down in the later stages of AD, and its association with the DMN A subnetwork. Brain systems, such as hippocampal place cells or entorhinal grid cells, once considered dedicated to spatial computations, are gradually recognized for their role in social cognition (Omer et al., 2018; Park et al., 2021). In an aforementioned study, Tavares et al. (2015) have shown that hippocampal BOLD signal during social “navigation” in the dimensions of power and affiliation was negatively correlated with social avoidance and neuroticism, suggesting a link between social orientation and interpersonal traits. Here, we present evidence suggesting that a relative preservation of social orientation in early stages of AD (followed by late disruption) is linked to relatively late neurodegeneration in the DMN A subnetwork regions. In the context of studies mapping social orientation to MTL structures, our results suggest that in addition to previously reported MTL regions, frontoparietal DMN-A regions play a critical role in social orientation.

To the best of our knowledge, ours is the first study to utilize a combination of PET and MR imaging to simultaneously assess neurodegeneration, task-induced brain activity, and performance within a single cohort. Regional cerebral hypometabolism in older adults has been considered a proxy of neurodegeneration, specifically synaptic dysfunction, which is thought to precede volume loss visualized by structural MRI and relate to early clinical manifestations of AD (Lan et al., 2022). As such, we hypothesized that hypometabolism measured by FDG-PET may mediate the association between brain activity and orientation performance. We used mediation analysis to jointly analyze functional, metabolic, and behavioral data, to examine whether (and where in the brain) hypometabolism mediates the relationship between orientation-evoked activity and task performance along the AD continuum. We conducted mediation analyses separately for spatio-temporal and social orientation, as well as for a lexical control task, matching the orientation task in format and stimuli yet differing in its cognitive requirements. For spatio-temporal and social orientation, mediation effects were found to be significant in DMN C and DMN A medial regions, respectively, suggesting AD-related neurodegeneration induces changes beyond simply suppressing activity and disrupting performance, but rather affecting the relations

between activity and performance (Huijbers et al., 2015). Taken together, these 3-layered data (orientation-evoked activity, orientation performance, and disease state reflected in hypometabolism) suggest that disorientation is disturbed according to pathology progression. Likewise, in early stages disease pathology propagates along a poster–anterior pathway, affecting spatio-temporal orientation, which overlaps mostly DMN C, both in the medial and lateral walls. In later stages, pathology advances to affect also more anterior regions, including the precuneus which processes social orientation, included in DMN A, but also involving the core orientation region in the lateral wall.

Additional studies have shown mixed patterns of hypo- and hyperactivation in patients along the AD spectrum (Foster et al., 2018; O'Brien et al., 2010). In one such study, Kunz et al. (2015) demonstrated that young asymptomatic APOE- ϵ 4 carriers (AD risk multiplier) exhibit decreased entorhinal and increased hippocampal activity while navigating a 3D arena. Exploring later, clinically detectable stages of AD, O'Brien et al. (2010) administered a memory-encoding task to a group of aMCI and older adult control participants while undergoing fMRI. The results demonstrated that while both groups were similarly successful in recall, stronger hippocampal activation in the aMCI group during encoding correlated to a higher rate of cognitive decline and sequential hypoactivation in follow-up scans. The effects of AD on brain activity therefore appear to relate both to the stage of the disease and to the task itself. Subsequent studies re-evaluated DMN neuroimaging markers of AD pathology.

Our results and conclusion notwithstanding, this work is not free from limitations. First, in recent years there has been a push for progressively shifting the definition of AD from a syndromal to a biological one (Jack et al., 2018). Specifically, AD biomarkers, including A β , tau, and neurodegeneration, have been reorganized into the ATN framework (Kern et al., 2018). In the current study, we focused on two separate markers of neurodegeneration, which were available to us: structural MRI and FDG-PET. In future studies, we intend to incorporate A β and tau PET imaging in order to shift the focus from networks and activity to pathology. Additionally, the current study was cross-sectional and had a relatively small sample size. Especially, only 12 patients with AD dementia participated in the study, due to the difficulty in finding such patients who are not too impaired and can still undergo fMRI paradigms reliably. Notably, our mediation analysis was agnostic to the specific diagnosis, considering the entire cohort as 51 participants along the AD continuum. Future studies will consist of larger sample sizes and longitudinal follow-up, allowing us to better understand the directionality of these brain–behavior associations and their evolution over time in AD.

In conclusion, this study demonstrates the central role of disorientation in AD and specifically the potential of evaluating orientation in multiple domains to differentiate between disease stages. We suggest that the relative early vulnerability of spatial and temporal orientation (compared to social orientation) stems from its association with temporoparietal regions, which are affected in early stages of the disease. Comparably, the relative resilience of social orientation stems from its association with the frontoparietal cortex, which is affected

only in later stages of the disease. We attribute these associations to distinct underlying computations performed by functionally distinct subnetworks of the DMN. We suggest that in parallel with the rapidly evolving evidence in support of usage of biomarkers in AD diagnosis, establishing a data-driven neurocognitive profile of AD degeneration will greatly benefit disease diagnosis, monitoring, and evaluation of treatment response.

AUTHOR CONTRIBUTIONS

Gregory Peters-Founshstein: Conceptualization; methodology; participant recruitment; investigation; data analysis; writing—original draft preparation; and writing—review and editing. Lidor Gazit: Participant recruitment; investigation; data analysis; writing—original draft preparation; and writing—review and editing. Tahel Naveh: participant recruitment; investigation; data analysis; and writing—original draft preparation. Liran Domachevsky: diagnostic imaging interpretation and writing—review and editing. Amos D. Korczyn: Participant recruitment; clinical diagnosis; and writing—review and editing. Hanna Bernstine: Diagnostic imaging interpretation and writing—review and editing. Limor Shaharabani-Gargir: Methodology and participant recruitment. David Groshar: Diagnostic imaging interpretation; writing—review and editing; and funding. Gad A. Marshall: Methodology; data analysis; and writing—review and editing. Shahar Arzy: Conceptualization; methodology; participant recruitment; clinical diagnosis, investigation; data analysis; writing—original draft preparation; writing—review and editing; and funding.

ACKNOWLEDGEMENTS

We are grateful to Mr. Zohar Nitsan, Ms. Inbal Machcat, and Mr. Hagai Baruch for their help in participant scanning and to Dr. Michael Peer, Dr. Moshe Roseman, Mr. Amnon Dafni-Merom, and Dr. Tal Sany-Ur for their insightful comments. This work was supported by the Israeli Science Foundation (grant no. 3213/19) and the NIH (grant no. R21 AG070877 to GAM, HS, and SA). SA is grateful to Mr. Ronald Abramson and the Glazer Foundation for their generous support.

CONFLICT OF INTEREST STATEMENT

The authors declare no conflicts of interest.

DATA AVAILABILITY STATEMENT

The data that support the findings of this study are available from the corresponding author upon reasonable request.

ORCID

Gregory Peters-Founshstein  <https://orcid.org/0000-0001-6874-1807>

REFERENCES

Albert, M. S., DeKosky, S. T., Dickson, D., Dubois, B., Feldman, H. H., Fox, N. C., Gamst, A., Holtzman, D. M., Jagust, W. J., Petersen, R. C., Snyder, P. J., Carrillo, M. C., Thies, B., & Phelps, C. H. (2011). The

diagnosis of mild cognitive impairment due to Alzheimer's disease: Recommendations from the National Institute on Aging-Alzheimer's Association workgroups on diagnostic guidelines for Alzheimer's disease. *Alzheimer's & Dementia*, 7(3), 270–279. <https://doi.org/10.1016/j.jalz.2011.03.008>

Andrews-Hanna, J. R., Reidler, J. S., Sepulcre, J., Poulin, R., & Buckner, R. L. (2010). Functional-anatomic fractionation of the brain's default network. *Neuron*, 65(4), 550–562. <https://doi.org/10.1016/j.neuron.2010.02.005>

Andrews-Hanna, J. R., Smallwood, J., & Spreng, R. N. (2014). The default network and self-generated thought: Component processes, dynamic control, and clinical relevance. *Annals of the New York Academy of Sciences*, 1316(1), 29–52. <https://doi.org/10.1111/nyas.12360>

Ashburner, J., & Friston, K. J. (2000). Voxel-based morphometry – The methods. *NeuroImage*, 11(6), 805–821. <https://doi.org/10.1006/nimg.2000.0582>

Barnett, A. J., Reilly, W., Dimsdale-Zucker, H. R., Mizrak, E., Reagh, Z., & Ranganath, C. (2021). Intrinsic connectivity reveals functionally distinct cortico-hippocampal networks in the human brain. *PLoS Biology*, 19, e3001275. <https://doi.org/10.1371/journal.pbio.3001275>

Barnett, D. A., Arnold, S. E., Valenzuela, M. J., Brayne, C., & Schneider, J. A. (2014). Cognition in late life. *Acta Neuropathologica*, 727(1), 137–150. <https://doi.org/10.1007/s00401-013-1226-2>

Bennett, D. A., Schneider, J. A., Tang, Y., Arnold, S. E., & Wilson, R. S. (2006). The effect of social networks on the relation between Alzheimer's disease pathology and level of cognitive function in old people: A longitudinal cohort study. *Lancet Neurology*, 5(5), 406–412. [https://doi.org/10.1016/S1474-4422\(06\)70417-3](https://doi.org/10.1016/S1474-4422(06)70417-3)

Berrios, G. E. (1982). Disorientation states and psychiatry. *Comprehensive Psychiatry*, 23(5), 479–491. [https://doi.org/10.1016/0010-440X\(82\)90161-4](https://doi.org/10.1016/0010-440X(82)90161-4)

Buckner, R. L., & DiNicola, L. M. (2019). The brain's default network: Updated anatomy, physiology and evolving insights. *Nature Reviews Neuroscience*, 20(10), 593–608. <https://doi.org/10.1038/s41583-019-0212-7>

Buckner, R. L., Snyder, A. Z., Shannon, B. J., LaRossa, G., Sachs, R., Fotenos, A. F., Sheline, Y. I., Klunk, W. E., Mathis, C. A., Morris, J. C., & Mintun, M. A. (2005). Molecular, structural, and functional characterization of Alzheimer's disease: Evidence for a relationship between default activity, amyloid, and memory. *Neuroscience*, 25(34), 7709–7717. <https://doi.org/10.1523/JNEUROSCI.2177-05.2005>

Busche, M. A., & Hyman, B. T. (2020). Synergy between amyloid- β and tau in Alzheimer's disease. *Nature Neuroscience*, 23(10), 1183–1193. <https://doi.org/10.1038/s41593-020-0687-6>

Byrne, P., Becker, S., & Burgess, N. (2007). Remembering the past and imagining the future: A neural model of spatial memory and imagery. *Psychological Review*, 114(2), 340–375. <https://doi.org/10.1037/0033-295X.114.2.340>

Coughlan, G., Coutrot, A., Khondoker, M., Minihane, A. M., Spiers, H., & Hornberger, M. (2019). Toward personalized cognitive diagnostics of at-genetic-risk Alzheimer's disease. *Proceedings of the National Academy of Sciences of the United States of America*, 116(19), 9285–9292. <https://doi.org/10.1073/pnas.1901600116>

Coughlan, G., Laczó, J., Hort, J., Minihane, A. M., & Hornberger, M. (2018). Spatial navigation deficits – Overlooked cognitive marker for preclinical Alzheimer disease? *Nature Reviews Neurology*, 14, 496–506. <https://doi.org/10.1038/s41582-018-0031-x>

Crary, J. F., Trojanowski, J. Q., Schneider, J. A., Abisambra, J. F., Abner, E. L., Alafuzoff, I., Arnold, S. E., Attems, J., Beach, T. G., Bigio, E. H., Cairns, N. J., Dickson, D. W., Gearing, M., Grinberg, L. T., Hof, P. R., Hyman, B. T., Jellinger, K., Jicha, G. A., Kovacs, G. G., ... Nelson, P. T. (2014). Primary age-related tauopathy (PART): A common pathology associated with human aging. *Acta Neuropathologica*, 128(6), 755–766. <https://doi.org/10.1007/s00401-014-1349-0>

- Dafni-Merom, A., Peters-Founshstein, G., Kahana-Merhavi, S., & Arzy, S. (2019). A unified brain system of orientation and its disruption in Alzheimer's disease. *Annals of Clinical and Translational Neurology*, 6(12), 2468–2478. <https://doi.org/10.1002/acn3.50940>
- Delpolyi, A. R., Rankin, K. P., Mucke, L., Miller, B. L., & Gorno-Tempini, M. L. (2007). Spatial cognition and the human navigation network in AD and MCI. *Neurology*, 69, 986–997.
- Du, M., Basyouni, R., & Parkinson, C. (2021). How does the brain navigate knowledge of social relations? Testing for shared neural mechanisms for shifting attention in space and social knowledge. *NeuroImage*, 235, 118019. <https://doi.org/10.1016/j.neuroimage.2021.118019>
- Dubois, B., Slachevsky, a., Litvan, I., & Pillon, B. (2000). The FAB: A frontal assessment battery at bedside. *Neurology*, 55(11), 1621–1626. <https://doi.org/10.1212/WNL.57.3.565>
- Foster, C. M., Kennedy, K. M., Horn, M. M., Hoagey, D. A., & Rodrigue, K. M. (2018). Both hyper- and hypo-activation to cognitive challenge are associated with increased beta-amyloid deposition in healthy aging: A nonlinear effect. *NeuroImage*, 166, 285–292. <https://doi.org/10.1016/j.neuroimage.2017.10.068>
- Franzmeier, N., Neitzel, J., Rubinski, A., Smith, R., Strandberg, O., Ossenkoppele, R., Hansson, O., Ewers, M., & Alzheimer's Disease Neuroimaging Initiative (ADNI). (2020). Functional brain architecture is associated with the rate of tau accumulation in Alzheimer's disease. *Nature Communications*, 11(1), 347. <https://doi.org/10.1038/s41467-019-14159-1>
- Fredericks, C. A., Sturm, V. E., Brown, J. A., Hua, A. Y., Bilgel, M., Wong, D. F., Resnick, S. M., & Seeley, W. W. (2018). Early affective changes and increased connectivity in preclinical Alzheimer's disease. *Alzheimer's and Dementia: Diagnosis, Assessment and Disease Monitoring*, 10, 471–479. <https://doi.org/10.1016/j.dadm.2018.06.002>
- Hachinski, V. C., Iliff, L. D., Zilhka, E., Du Boulay, G. H., McAllister, V. L., Marshall, J., Russell, R. W. R., & Symon, L. (1975). Cerebral blood flow in dementia. *Archives of Neurology*, 32(9), 632–637.
- Hayman, M., & Arzy, S. (2021). Mental travel in the person domain. *Journal of Neurophysiology*, 20(7), 464–476. <https://doi.org/10.1152/jn.00695.2020>
- Huijbers, W., Mormino, E. C., Schultz, A. P., Wigman, S., Ward, A. M., Larvie, M., Amariglio, R. E., Marshall, G. A., Rentz, D. M., Johnson, K. A., & Sperling, R. A. (2015). Amyloid- β deposition in mild cognitive impairment is associated with increased hippocampal activity, atrophy and clinical progression. *Brain*, 138(4), 1023–1035. <https://doi.org/10.1093/brain/awv007>
- Jack, C. R., Jr., Bennett, D. A., Blennow, K., Carrillo, M. C., Dunn, B., Haeberlein, S. B., Holtzman, D. M., Jagust, W., Jessen, F., Karlawish, J., Liu, E., Molinuevo, J. L., Montine, T., Phelps, C., Rankin, K. P., Rowe, C. C., Scheltens, P., Siemers, E., Snyder, H. M., ... Contributors. (2018). NIA-AA research framework: Toward a biological definition of Alzheimer's disease. *Alzheimer's & Dementia*, 14(4), 535–562. <https://doi.org/10.1016/j.jalz.2018.02.018>
- Kanda, T., Ishii, K., Uemura, T., Miyamoto, N., Yoshikawa, T., Kono, A. K., & Mori, E. (2008). Comparison of grey matter and metabolic reductions in frontotemporal dementia using FDG-PET and voxel-based morphometric MR studies. *European Journal of Nuclear Medicine and Molecular Imaging*, 35(12), 2227–2234. <https://doi.org/10.1007/s00259-008-0871-5>
- Kaplan, R., & Friston, K. J. (2018). Entorhinal transformations in abstract frames of reference. *PLOS Biology*, 17(5), e3000230. <https://doi.org/10.1371/journal.pbio.3000230>
- Kern, S., Zetterberg, H., Kern, J., Zettergren, A., Waern, M., Höglund, K., Andreasson, U., Wetterberg, H., Börjesson-Hanson, A., Blennow, K., & Skoog, I. (2018). Prevalence of preclinical Alzheimer disease: Comparison of current classification systems. *Neurology*, 90(19), E1682–E1691. <https://doi.org/10.1212/WNL.0000000000005476>
- Kunz, L., Schröder, T. N., Lee, H., Montag, C., Lachmann, B., Sariyska, R., Reuter, M., Stürmberg, R., Stöcker, T., Messing-Floeter, P. C., Fell, J., Doeller, C. F., & Axmacher, N. (2015). Reduced grid-cell-like representations in adults at genetic risk for Alzheimer's disease. *Science*, 350(6259), 430–433. <https://doi.org/10.1126/science.aac8128>
- Lan, G., Cai, Y., Li, A., Liu, Z., Ma, S., Guo, T., & Alzheimer's Disease Neuroimaging Initiative. (2022). Association of presynaptic loss with Alzheimer's disease and cognitive decline. *Annals of Neurology*, 92(6), 1001–1015.
- Lin, C., Ly, M., Karim, H. T., Wei, W., Snitz, B. E., Klunk, W. E., & Aizenstein, H. J. (2020). The effect of amyloid deposition on longitudinal resting-state functional connectivity in cognitively normal older adults. *Alzheimer's Research & Therapy*, 12(1), 1–10. <https://doi.org/10.1186/s13195-019-0573-1>
- Mahendran, R., Chua, J., Feng, L., Kua, E. H., & Preedy, V. R. (2015). The mini-mental state examination and other neuropsychological assessment tools for detecting cognitive decline. In C. R. Martin & V. R. Preedy (Eds.), *Diet and nutrition in dementia and cognitive decline* (pp. 1159–1174). Academic Press. <https://doi.org/10.1016/B978-0-12-407824-6.00109-9>
- Marcus, C., Mena, E., & Subramaniam, R. M. (2014). Brain PET in the Diagnosis of Alzheimer's Disease. *Clinical Nuclear Medicine*, 39(10), e413–e426. <https://doi.org/10.1097/rlu.0000000000000547>
- Mathuranath, P. S., Nestor, P. J., Berrios, G. E., Rakowicz, W., & Hodges, J. R. (2000). A brief cognitive test battery to differentiate Alzheimer's disease and frontotemporal dementia. *Neurology*, 55(11), 1613–1620.
- McKhann, G. M., Knopman, D. S., Chertkow, H., Hyman, B. T., Jack, C. R., Jr., Kawas, C. H., Klunk, W. E., Koroshetz, W. J., Manly, J. J., Mayeux, R., Mohs, R. C., Morris, J. C., Rossor, M. N., Scheltens, P., Carrillo, M. C., Thies, B., Weintraub, S., & Phelps, C. H. (2011). The diagnosis of dementia due to Alzheimer's disease: Recommendations from the National Institute on Aging-Alzheimer's Association workgroups on diagnostic guidelines for Alzheimer's disease. *Alzheimer's & Dementia*, 7(3), 263–269. <https://doi.org/10.1016/j.jalz.2011.03.005>
- Morris, J. C. (1993). The clinical dementia rating (CDR): Current version and scoring rules. *Neurology*, 43(11), 2412–2414. <https://doi.org/10.1212/WNL.43.11.2412-a>
- Nasreddine, Z. S., Phillips, N. A., Bédirian, V., Charbonneau, S., Whitehead, V., Collin, I., Cummings, J. L., & Chertkow, H. (2005). The Montreal Cognitive Assessment, MoCA: A brief screening tool for mild cognitive impairment. *Journal of the American Geriatrics Society*, 53(4), 695–699. <https://doi.org/10.1111/j.1532-5415.2005.53221.x>
- O'Brien, J. L., O'Keefe, K. M., Laviolette, P. S., Deluca, A. N., Blacker, D., Dickerson, B. C., & Sperling, R. A. (2010). Longitudinal fMRI in elderly reveals loss of hippocampal activation with clinical decline. *Neurology*, 74(24), 1969–1976. <https://doi.org/10.1212/WNL.0b013e3181e3966e>
- Omer, D. B., Maimon, S. R., Las, L., & Ulanovsky, N. (2018). Social place-cells in the bat hippocampus. *Science*, 359(6372), 218–224. <https://doi.org/10.1126/science.aao3474>
- Palmqvist, S., Schöll, M., Strandberg, O., Mattsson, N., Stomrud, E., Zetterberg, H., Blennow, K., Landau, S., Jagust, W., & Hansson, O. (2017). Earliest accumulation of β -amyloid occurs within the default-mode network and concurrently affects brain connectivity. *Nature Communications*, 8(1), 1–13. <https://doi.org/10.1038/s41467-017-01150-x>
- Park, S. A., Miller, D. S., & Boorman, E. D. (2021). Inferences on a multidimensional social hierarchy use a grid-like code. *Nature Neuroscience*, 24(9), 1292–1301. <https://doi.org/10.1038/s41593-021-00916-3>
- Peer, M., Salomon, R., Goldberg, I., Blanke, O., & Arzy, S. (2015). Brain system for mental orientation in space, time, and person. *Proceedings of the National Academy of Sciences of the United States of America*, 112(35), 11072–11077. <https://doi.org/10.1073/pnas.1504242112>

- Peters-Founshtein, G., Peer, M., Rein, Y., Kahana Merhavi, S., Meiner, Z., & Arzy, S. (2018). Mental-orientation: A new approach to assessing patients across the Alzheimer's disease spectrum. *Neuropsychology*, 32, 690–699. <https://doi.org/10.1037/neu0000463>
- Rapoport, B. I., & Rapoport, S. (2015). Orientation to person, orientation to self. *Neurology*, 85(23), 2072–2074. <https://doi.org/10.1212/WNL.0000000000002188>
- Sabat, S. R., & Lee, J. M. (2012). Relatedness among people diagnosed with dementia: Social cognition and the possibility of friendship. *Dementia*, 11(3), 315–327. <https://doi.org/10.1177/1471301211421069>
- Schaefer, A., Kong, R., Gordon, E. M., Laumann, T. O., Zuo, X. N., Holmes, A. J., Eickhoff, S. B., & Yeo, B. T. T. (2018). Local-global parcellation of the human cerebral cortex from intrinsic functional connectivity MRI. *Cerebral Cortex*, 28(9), 3095–3114. <https://doi.org/10.1093/cercor/bhx179>
- Schafer, M., & Schiller, D. (2018). Navigating social space. *Neuron*, 100(2), 476–489. <https://doi.org/10.1016/j.neuron.2018.10.006>
- Silson, E. H., Steel, A., Kidder, A., Gilmore, A. W., & Baker, C. I. (2019). Distinct subdivisions of human medial parietal cortex support recollection of people and places. *eLife*, 8, e47391. <https://doi.org/10.1101/554915>
- Sturm, V. E., Yokoyama, J. S., Seeley, W. W., Kramer, J. H., Miller, B. L., & Rankin, K. P. (2013). Heightened emotional contagion in mild cognitive impairment and Alzheimer's disease is associated with temporal lobe degeneration. *Proceedings of the National Academy of Sciences of the United States of America*, 110(24), 9944–9949. <https://doi.org/10.1073/pnas.1301119110>
- Tavares, R. M., Mendelsohn, A., Grossman, Y., Williams, C. H., Shapiro, M., Trope, Y., & Schiller, D. (2015). A map for social navigation in the human brain. *Neuron*, 87(1), 231–243.
- Townsend, J. T., & Ashby, F. G. (1983). Stochastic modeling of elementary psychological processes. *The American Journal of Psychology*, 480, 480. <https://doi.org/10.2307/1422636>
- van der Kant, R., Goldstein, L. S. B., & Ossenkuppele, R. (2020). Amyloid- β -independent regulators of tau pathology in Alzheimer disease. *Nature Reviews Neuroscience*, 21, 21–35. <https://doi.org/10.1038/s41583-019-0240-3>
- Whittington, J. C. R., McCaffary, D., Bakermans, J. J. W., & Behrens, T. E. J. (2022). How to build a cognitive map. *Nature Neuroscience*, 25(10), 1257–1272. <https://doi.org/10.1038/s41593-022-01153-y>
- Worsley, K. J., & Friston, K. J. (1995). Analysis of fMRI time-series revisited – Again. *NeuroImage*, 2(3), 173–181. <https://doi.org/10.1006/nimg.1995.1023>

SUPPORTING INFORMATION

Additional supporting information can be found online in the Supporting Information section at the end of this article.

How to cite this article: Peters-Founshtein, G., Gazit, L., Naveh, T., Domachevsky, L., Korczyn, A. D., Bernstine, H., Shaharabani-Gargir, L., Groshar, D., Marshall, G. A., & Arzy, S. (2024). Lost in space(s): Multimodal neuroimaging of disorientation along the Alzheimer's disease continuum. *Human Brain Mapping*, 45(4), e26623. <https://doi.org/10.1002/hbm.26623>